

Evidence of a first-order smectic-hexatic transition and its proximity to a tricritical point in smectic films

Ivan A. Zaluzhnyy,^{1,2} Ruslan P. Kurta,³ Nastasia Mukharamova,¹ Young Yong Kim,¹ Ruslan M. Khubbutdinov,^{1,2,4} Dmitry Dzhigaev,¹ Vladimir V. Lebedev,^{5,6} Elena S. Pikina,^{4,5,*} Efim I. Kats,⁵ Noel A. Clark,^{7,8} Michael Sprung,¹ Boris I. Ostrovskii,^{4,9,†} and Ivan A. Vartanyants^{1,2,‡}

¹Deutsches Elektronen-Synchrotron DESY, Notkestraße 85, D-22607 Hamburg, Germany

²National Research Nuclear University MEPhI (Moscow Engineering Physics Institute), Kashirskoe shosse 31, 115409 Moscow, Russia

³European XFEL GmbH, Holzkoppel 4, D-22869 Schenefeld, Germany

⁴Institute of Solid State Physics, Russian Academy of Sciences, Academician Ossipyan str. 2, 142432 Chernogolovka, Russia

⁵Landau Institute for Theoretical Physics, Russian Academy of Sciences, pr. akademika Semenova 1-A, 142432 Chernogolovka, Russia

⁶National Research University Higher School of Economics, Myasnitskaya ul. 20, 101000 Moscow, Russia

⁷Department of Physics, University of Colorado Boulder, Boulder, Colorado 80309, USA

⁸Soft Materials Research Center, University of Colorado Boulder, Boulder, Colorado 80309, USA

⁹Federal Scientific Research Center “Crystallography and photonics”, Russian Academy of Sciences, Leninskii prospect 59, 119333 Moscow, Russia



(Received 1 June 2018; published 16 November 2018)

Experimental and theoretical studies of a smectic-*A*–hexatic-*B* transition in freely suspended films of thickness 2–10 μm of the *n*-pentyl-4′-*n*-pentanoyloxy-biphenyl-4-carboxylate (54COOBC) compound are presented. X-ray investigations revealed a discontinuous first-order transition into the hexatic phase. The temperature region of two-phase coexistence near the phase transition point diminishes with decreasing film thickness. The width of this temperature region as a function of the film thickness was derived on the basis of a Landau mean-field theory in the vicinity of a tricritical point (TCP). Close to TCP the surface hexatic-*B* order penetrates anomalously deep into the film interior.

DOI: [10.1103/PhysRevE.98.052703](https://doi.org/10.1103/PhysRevE.98.052703)

I. INTRODUCTION

Phase transitions are one of the richest and most intriguing phenomena in modern physics [1,2]. Despite important progress in understanding of the origin and fluctuation behavior of various systems, the topic still presents many challenging open questions. Among them, of special interest, are the anomalous behavior and remarkable material properties of the systems in the vicinity of the tricritical point (TCP), where the phase transition changes from second to first order. This includes a study of TCPs in a variety of systems such as liquid crystals (LCs) [3], colloidal crystals [4], and block copolymers [5–7]. The presence of TCP has been proved and extensively studied in LC mixtures for the nematic to smectic-*A* (Sm-*A*) transition [8–10]. A great impact on the development of this field provided a recent discovery of fluctuation-induced TCPs in skyrmionic magnetic lattices [11–13]. Liquid-crystal freely suspended films (FSFs) are particularly suitable to investigate the above problems: such films are substrate-free; the alignment of the smectic layers is almost perfect, allowing the study of single-domain samples of various thickness [14,15]. The FSFs have provided an ideal model system for studying the effects of finite-size,

surface-induced ordering, and their influence on the LC phase transitions in the vicinity of the TCP.

Here we report on the behavior of the first-order Sm-*A*–hexatic-*B* (Hex-*B*) phase transition in LCs and find that it can be tuned close to a TCP by film thickness variation. The Hex-*B* is a three-dimensional (3D) analog of the common hexatic phase [16–18]. It can be considered as a stack of parallel molecular layers, in which elongated molecules are oriented on average along the layer normals, exhibiting long-range bond-orientational (BO) order and short-range positional order within each layer [19–21].

Despite three decades of intensive studies, understanding of the Sm-*A*–Hex-*B* phase transition is still limited not only in details but even conceptually. According to the Landau theory of phase transitions [3,22], this transition is characterized by the two-component BO order parameter $\psi = |\psi| \exp(i6\phi)$ (modulus and phase) and therefore the continuous phase transition must follow the universal behavior predicted for such a case. In reality, a number of experiments [15,21,23–26] do not support this concept demanding a revision of this simple picture. This has become especially important recently as experiments (x-ray diffraction and calorimetry) grow in resolution and sophistication [25–28].

Here we perform a detailed x-ray study, enabled by a synchrotron-based coherent photon source, of tricritical behavior in the LC-forming material 54COOBC (*n*-pentyl-4′-*n*-pentanoyloxy-biphenyl-4-carboxylate) which exhibits a Sm-*A*–Hex-*B* phase transition that depends on the effective

*Corresponding author: elenapikina@itp.ac.ru

†Corresponding author: ostrenator@gmail.com

‡Corresponding author: ivan.vartanyants@desy.de

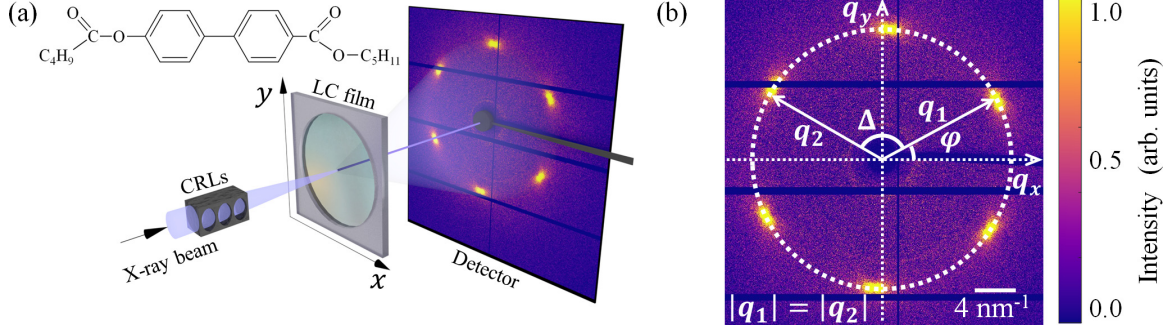


FIG. 1. (a) Schematic representation of x-ray diffraction setup used in the experiment. The x-ray beam is focused by CRLs. The freestanding LC film is oriented perpendicular to the incoming beam, and piezoelectric motors allow one to scan the film in the XY plane. The diffraction pattern is recorded in transmission geometry by an EIGER 4M detector placed behind the LC film. The direct beam is blocked by a beamstop. The chemical structure of the 54COOBC compound is shown in the inset. (b) Example of the diffraction pattern from the Hex- B phase and polar coordinate system for evaluation of the angular cross-correlation function $G(q, \Delta)$.

dimensionality of the sample. In bulk it has the following phase sequence: I (70 °C) Sm- A (55 °C) Hex- B (53 °C) Cr- B , where I stays for the isotropic phase and Cr for crystal phase, respectively [29–32]. A first-order Sm- A –Hex- B phase transition occurs in bulk samples [23,29], while very thin FSFs show a continuous Sm- A –Hex- B phase transition [30,31]. It was argued [31] that this smectic–hexatic phase transition in two-layered 54COOBC films occurs via an intermediate Sm- A' phase, which is characterized by absence of the BO order and increased in-layer positional correlation as compared to the common Sm- A phase. In bulk samples the first-order Sm- A –Hex- B phase transition lies in the vicinity of a TCP. We show that near this TCP the surface ordering penetrates anomalously deep into the interior of the film, which essentially influences the Sm- A –Hex- B phase transition even for thick films, consisting of thousands of layers.

II. EXPERIMENT

A. Sample preparation and experimental setup

The freely suspended smectic films of 54COOBC [see the inset in Fig. 1(a) for the chemical structure] were drawn across a circular hole of 2 mm in diameter in a thin glass plate [25,26,33]. By varying the temperature and speed of drawing, one can produce films of various thickness, which was measured using an Avantes fiber optic spectrometer. The films were placed inside a FS1 sample stage from Instec connected to an mK1000 temperature controller. The accuracy of temperature control during experiment was about 0.005 °C.

X-ray studies were performed using 13 keV photons (wavelength of 0.954 Å) at the coherence beamline P10 of PETRA III synchrotron source at DESY [Fig. 1(a)]. The films were positioned perpendicular to the incident x-ray beam, which was focused by compound refractive lenses (CRLs) to the size of about $2 \times 2 \mu\text{m}^2$ at full width at half maximum. The scattering signal was recorded by an EIGER 4M detector (2070×2167 pixels of $75 \times 75 \mu\text{m}^2$ size) placed 232 mm behind the sample. At each temperature the film was scanned with an x-ray beam over an area $100 \times 100 \mu\text{m}^2$ with a step of $5 \mu\text{m}$. Each diffraction pattern was collected at an exposure time of 0.5 s to avoid radiation damage of the film. Prior to further analysis the collected diffraction patterns were

corrected for background scattering and horizontal polarization of synchrotron radiation.

B. Angular x-ray cross-correlation analysis

In this work we used angular x-ray cross-correlation analysis (XCCA) for direct evaluation of the BO order parameters in the Hex- B phase. XCCA is a technique that allows one to study local angular order present in a system by analysis of the angular distribution of the scattered intensity [34–37]. The key element of XCCA is the two-point angular correlation function evaluated for each diffraction pattern [35,37]

$$G(q_1, q_2, \Delta) = \langle I(q_1, \varphi) I(q_2, \varphi + \Delta) \rangle_{\varphi}. \quad (1)$$

Here (q, φ) are polar coordinates at the detector plane, Δ is the angular variable, and $\langle \dots \rangle_{\varphi}$ denotes averaging over azimuthal angle φ [see Fig. 1(b)]. In this work we used the momentum transfer value $q_0 = q_1 = q_2$, where q_0 is a position of the maximum of the scattered intensity. Information about the rotational symmetry of the diffraction pattern is contained in the cross-correlation function defined in Eq. (1) and can be easily analyzed by utilizing angular Fourier components

$$G_n(q) = \frac{1}{2\pi} \int_0^{2\pi} G(q, \Delta) \exp^{-in\Delta} d\Delta. \quad (2)$$

It can be shown [35] that the values of Fourier components $G_n(q)$ are directly related to the angular Fourier components of intensity

$$I_n(q) = \frac{1}{2\pi} \int_0^{2\pi} I(q, \varphi) \exp^{-in\varphi} d\varphi \quad (3)$$

as

$$G_n(q) = |I_n(q)|^2. \quad (4)$$

The angular cross-correlation function $G(q, \Delta)$ as well as its Fourier components $G_n(q)$ can be averaged over an ensemble of diffraction patterns to obtain representative information about the sample and improve signal-to-noise ratio. In contrast, one cannot average individual diffraction patterns or Fourier components of intensity $I_n(q)$, as soon as the angular position of the peaks may vary from pattern to pattern [26,33].

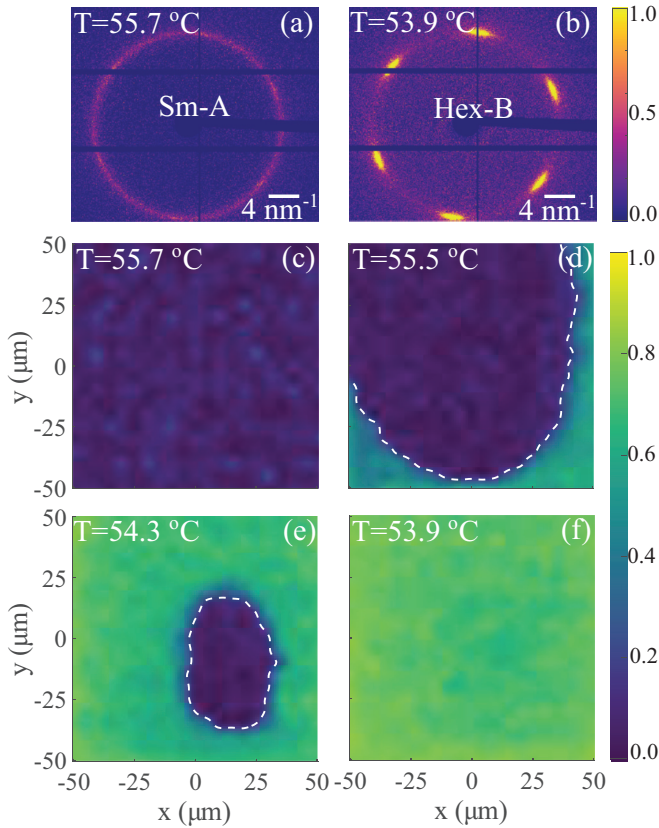


FIG. 2. [(a),(b)] Examples of diffraction patterns from 10- μm -thick film in the Sm-*A* (a) and Hex-*B* (b) phases of 54COOBC. Each image is averaged over 16 diffraction patterns collected within the area of $20 \times 20 \mu\text{m}^2$ for better visibility. Color refers to the normalized intensity of the scattered x rays. [(c)–(f)] Spatially resolved maps of BO order parameter C_6 in a $100 \times 100 \mu\text{m}^2$ region of the 54COOBC film in the Sm-*A* phase (c), mixed state (d),(e), and Hex-*B* phase (f). Color indicates the local value of C_6 : blue (dark) color corresponds to the Sm-*A* phase, and green (bright) corresponds to Hex-*B*. The dashed white line marks a border between the Sm-*A* and Hex-*B* phases in (d) and (e).

Such averaging may lead to angular smearing of the diffraction peaks, or even produce an angular isotropic pattern, that will result in loss of information about the orientational order contained in individual diffraction patterns.

III. RESULTS

The FSFs of different thickness ranging from 2 to 10 μm were measured on cooling and heating to observe the formation of the hexatic phase at the Sm-*A*–Hex-*B* phase transition. Examples of the measured diffraction patterns in the Sm-*A* and Hex-*B* phases are shown in Figs. 2(a) and 2(b). The diffraction pattern in the Sm-*A* phase [Fig. 2(a)] shows a typical for liquids broad scattering ring centered at a scattering momentum transfer value $q_0 \approx 4\pi/a\sqrt{3} \approx 14\text{nm}^{-1}$, where $a \approx 0.5 \text{ nm}$ is the average in-plane intermolecular distance [15,26]. In the Hex-*B* phase [Fig. 2(b)] one can readily see sixfold modulation of the in-plane scattering, which is evidence of the developing BO order.

To quantitatively describe the magnitude of the angular modulation of intensity in the Hex-*B* phase we used the BO order parameters C_{6m} (m is an integer). They are defined as a normalized amplitude of the sixfold angular Fourier components of the azimuthal scattered intensity [20,25]. The values of C_{6m} can be conveniently determined using the angular XCCA, which allows one to evaluate C_{6m} directly from the measured x-ray diffraction patterns [25,33,37]

$$C_{6m} = \left| \frac{I_{6m}(q_0)}{I_0(q_0)} \right| = \sqrt{\frac{G_{6m}(q_0)}{G_0(q_0)}}, \quad (5)$$

where all angular Fourier components are calculated over the ring with the radius q_0 . By definition, the value of the BO order parameter is normalized, $0 \leq C_{6m} \leq 1$; in the Sm-*A* phase $C_{6m} = 0$ for all integer m , while in the Hex-*B* phase the BO order parameters C_{6m} successively attains nonzero values upon temperature decrease [26,33,38]. In this work we analyzed temperature dependence of the fundamental BO order parameter C_6 , which is sufficient to distinguish Sm-*A* and Hex-*B* phases, while analysis of higher components C_{6m} providing more detailed information of the BO order will be the subject of a future publication.

Utilizing a microfocused x-ray beam, the spatially resolved maps were measured to reveal spatial variation of the BO order parameter C_6 within the scanned area. These maps for 10- μm -thick FSF for different temperatures while cooling are shown in Figs. 2(c)–2(f). At high temperature [Fig. 2(c)] the whole FSF is in the Sm-*A* phase; however, at lower temperatures the film becomes nonuniform. The coexistence of the Sm-*A* and Hex-*B* phases can be clearly seen in Figs. 2(d) and 2(e). The Hex-*B* phase coexists with the Sm-*A* phase [Fig. 2(d)] and then, at even lower temperatures, Hex-*B* becomes dominant and the Sm-*A* phase exists in the form of regions surrounded by the Hex-*B* phase [Fig. 2(e)]. The size, shape, and position of these regions may change when temperature varies; however, we always observed the Sm-*A* phase surrounded by the Hex-*B* phase in different films of 54COOBC, both on cooling and heating. This observation can be explained by the fact that above the bulk Sm-*A*–Hex-*B* phase transition temperature, the hexatic order is first formed at the surface of the film and it penetrates into the inner layers on cooling [15,23,39]. For such a mechanism of the Hex-*B* phase formation, the appearance of the Sm-*A* regions is favorable, contrary to the nucleation process, for which islands of the Hex-*B* phase surrounded by the Sm-*A* phase should be observed. During further cooling of the whole FSF turns to the Hex-*B* phase with the formation of single hexatic domains of a lateral size of hundreds of microns [Fig. 2(f)].

In order to perform an independent analysis of scattering from the Hex-*B* and Sm-*A* regions of the film one needs to find the criterion to distinguish between the Sm-*A* and Hex-*B* phases. Thus, theoretical criterion $C_6 = 0$ in Sm-*A* and $C_6 > 0$ in Hex-*B* does not work for real experimental data due to presence of noise in diffraction patterns, which leads to positive values of C_6 BO order parameter even in the Sm-*A* phase. To overcome this problem, a statistical analysis of C_6 values was performed, using diffraction patterns measured at different positions of LC film. It turned out that the fundamental BO order parameter C_6 in the uniform Sm-*A* phase

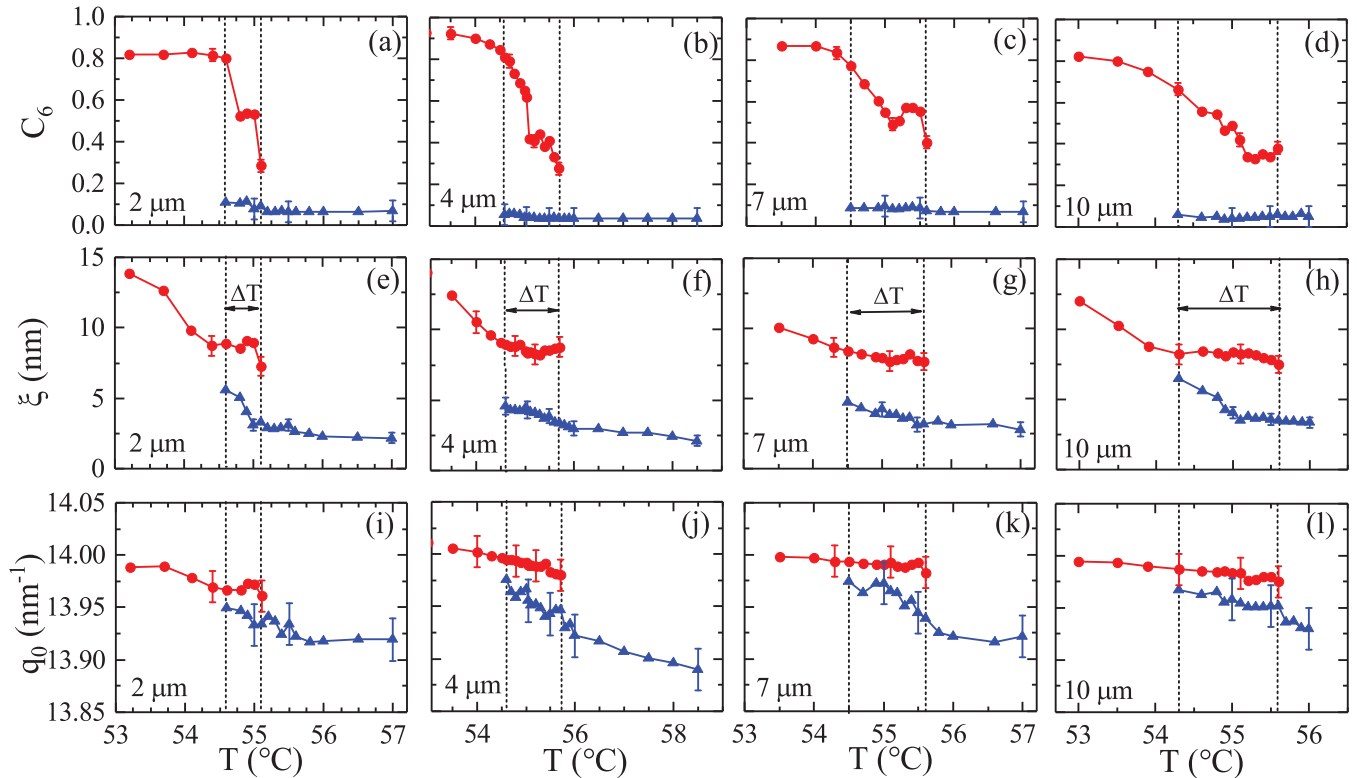


FIG. 3. Temperature dependence of the BO order parameter C_6 [(a)–(d)], positional correlation length ξ [(e)–(h)], and scattering peak maximum position q_0 [(i)–(l)] in the Sm-A phase (blue triangles) and Hex-B phase (red circles) close to the region of two-phase coexistence. Data are shown for 2- μm - [(a),(e),(i)], 4- μm - [(b),(f),(j)], 7- μm - [(c),(g),(k)], and 10- μm - [(d),(h),(l)] thick films of 54COOBC. The dashed vertical lines indicate the temperature region ΔT of two-phase coexistence. Error bars are shown for every fifth experimental point.

(measured at high temperature $T = 59^\circ\text{C}$) has a mean value of $\langle C_6 \rangle = 0.05$ and standard deviation $\delta C_6 = 0.04$. Based on this analysis, a threshold value $C_t = \langle C_6 \rangle + \delta C_6 = 0.09$ was introduced to separate Sm-A and Hex-B phases. Thus, each measured diffraction pattern at any temperature was attributed to one or another phase by following criterion: $C_6 \geq 0.09$ for Hex-B and $C_6 < 0.09$ for Sm-A. This criterion was used throughout the work to perform a separate analysis of Sm-A and Hex-B phases.

In Figs. 3(a)–3(d) the temperature dependence of the BO order parameter C_6 for the Sm-A (blue triangles) and Hex-B (red circles) phases for different film thicknesses is shown. This dependence was obtained by averaging the local values of C_6 calculated for each measured diffraction pattern over the regions of Sm-A and Hex-B phases separately [Figs. 2(c)–2(f)]. In the Sm-A phase the magnitude of C_6 is vanishingly small and does not change with the temperature. In the Hex-B phase the value of C_6 rises during cooling, which corresponds to an increase of the BO order in the low-temperature hexatic phase. As is expected for the first-order phase transition the BO order parameter does not change continuously from zero, but instead shows a discontinuous jump of the magnitude of about 0.3 at the temperature where the first areas of the hexatic phase appear in the film. These abrupt changes in values of the BO order parameter unambiguously determine the range of coexistence of the Sm-A and Hex-B phases in both films.

One of the important characteristics of the in-plane short-range order in smectic and hexatic phases is the positional

correlation length ξ , determining the length scale over which the positional correlations between the molecules decay [40]. In the Hex-B phase the value of positional correlation length can be calculated as $\xi = 1/\Delta q$, where Δq is a half width at half maximum (HWHM) of the radial cross section of the hexatic diffraction peak through its maximum. In the Sm-A phase the positional correlation length ξ can be evaluated in a similar way by using the HWHM of the radial cross section at the smectic scattering ring. In this work we evaluated Δq by fitting the radial intensity profile with Lorentzian function [33,40].

The temperature dependence of the positional correlation length averaged over regions of the Sm-A and Hex-B phases for different film thicknesses is shown in Figs. 3(e)–3(h). In the Sm-A phase the value of ξ gradually increases from approximately 2.5 nm at the temperature just above the phase transition to about 5 nm at the lowest temperature of the Sm-A phase coexistence. The discontinuity in ξ values at the borders of the two-phase region is a prime indication of the first-order character of the Sm-A–Hex-B transition in 54COOBC films. In the Hex-B phase the positional correlation length further increases on cooling until the crystal phase is formed. Such a behavior is attributed to coupling between the BO order and positional correlations in the Hex-B phase [33,41]. Although we did not observe any indications of Sm-A' phase in thick LC films, qualitatively the growth of the positional correlation length ξ within the two-phase region observed in our experiment resembles the range of enhanced values

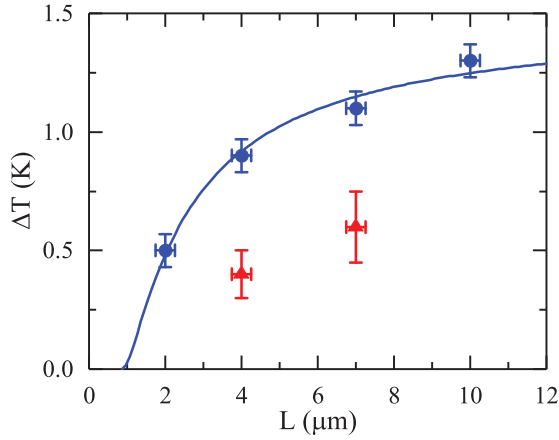


FIG. 4. Temperature range ΔT of the Sm-A and Hex-B phase coexistence (two-phase region) as a function of the film thickness L . Blue circles correspond to data taken on cooling and red triangles on heating of the 54COOBC films. Fitting of the data on cooling by Eq. (20) is shown by a solid line.

of the positional correlations reported earlier for a two-layer 54COOBC films [31].

Another important parameter characterizing the Sm-A–Hex-B phase transition is the position of the maximum of scattered intensity q_0 in the smectic and hexatic phases. The value of q_0 is inversely proportional to the average in-plane separation between LC molecules, and thus indicates the variation of density across the transition point. According to the theory of Aeppli and Bruinsma [41] the growth of fluctuations of the BO order parameter in the vicinity of a second-order Sm-A–Hex-B phase transition leads to a continuous increase of the peak’s maximum position q_0 and the appearance of an inflection point of $q_0(T)$ at the phase transition temperature. This is indeed observed for many LC compounds possessing a second-order Sm-A–Hex-B phase transition [26,33,42].

The situation becomes different for the first-order Sm-A–Hex-B phase transition, where one can expect a discontinuous density jump at the phase transition point. The discontinuity in q_0 at the borders of the two-phase region is readily seen in Figs. 3(i)–3(l), thus providing one more firm evidence for the first-order character of the Sm-A to Hex-B transition in 54COOBC films. The values of q_0 in both coexisting phases differ by about 0.4%, which is rather small for the structural phase transitions of the first order and can be explained by closeness of the system to the TCP.

An important outcome of our experiment was not only the observation of the coexistence of the Sm-A and Hex-B phases over a finite temperature range ΔT but also revealing its dependence on the film thickness (shown by blue circles in Fig. 4). We found that the width of the two-phase coexistence region is about 1.3 K for thick (10 μm) films and decreases for thinner films, reaching the value of about 500 mK for a film with a thickness of 2 μm . These observations are in good agreement with data reported for an approximately 0.25- μm -thick film (100 molecular layers) of 54COOBC compound, in which the coexistence of Sm-A and Hex-B phases was estimated to be within 90 mK [23,29]. The coexistence of two phases indicates that the average density of the film is

intermediate between that of the smectic and hexatic, thereby inducing two-phase equilibrium. Another important observation arising from our experiment is that the value of two-phase region ΔT obtained on cooling is larger than on heating (shown by red triangles in Fig. 4). Such behavior looks natural due to the presence of the hexatic surface ordering in the smectic phase. Thus the Sm-A phase cannot be overcooled, but contrary to that the Hex-B phase can be relatively easily overheated.

IV. THEORY

In the following we derive an analytical expression which models the temperature coexistence width as a function of film thickness. For theoretical analysis of our experimental results let us start with one of the general thermodynamical conditions of the equilibrium coexistence of the Sm-A and Hex-B phases in bulk (apart from the equality of the temperatures)

$$\mu_H[T, n_H] = \mu_{Sm}[T, n_{Sm}], \quad (6)$$

where $\mu_H[T, n_H] = \partial f_H[T, n_H]/\partial n_H$ and $\mu_{Sm}[T, n_{Sm}] = \partial f_{Sm}[T, n_{Sm}]/\partial n_{Sm}$ are the chemical potentials of the Hex-B and Sm-A phases, respectively, $f[T, n]$ is the free energy of the phase with density n (the number of molecules per unit volume for a fixed number of smectic layers), and indexes H and Sm correspond to the Hex-B and Sm-A phases, respectively. The possibility of the finite temperature interval for the two-phase coexistence suggests that neither of the phases can provide the correct density (only a combination of both phases). This is similar to liquid-vapor coexistence in the pressure-temperature coordinates. We designate as $\varphi[T, n]$ the free-energy density of the Sm-A phase per unit volume, $f_{Sm}[T, n_{Sm}] = \varphi[T, n_{Sm}]$. In the vicinity of the TCP the free-energy density f_H of the Hex-B phase (per unit volume) can be written according to conventional mean-field theory [22,43] as $f_H[T, n_H] = \varphi[T, n_H] + g[\psi]$, where

$$g[\psi] = a|\psi|^2 - \lambda|\psi|^4/6 + \zeta|\psi|^6/90 \quad (7)$$

is the Landau functional for the order parameter ψ (per unit volume) and a , λ , and ζ are Landau coefficients which depend on T and n . The coefficients a and λ are assumed to be small (they vanish at the TCP) and $\lambda > 0$ for a first-order transition. We consider a relatively narrow temperature interval where the Hex-B and Sm-A phases coexist. Therefore the coefficient ζ remains approximately constant in this interval, whereas coefficient a has a standard form [22,43] $a = \alpha\tau$, where $\alpha > 0$ is a constant and $\tau = (T - T_0)/T_0$. The coefficient a vanishes at a certain temperature T_0 which is in the vicinity of TCP close to the temperature of the bulk Sm-A–Hex-B phase transition [where straightforward analysis of the Landau functional (7) yields to $a_c = 5\lambda^2/8\zeta$, i.e., $\tau_c = 5\lambda^2/(8\alpha\zeta)$, $|\psi_c|^2 = 15\lambda/2\zeta$].

The order parameter ψ in the Hex-B phase is determined by minimization of expression (7):

$$|\psi_H|^2 = (5\lambda/\zeta)[1 + \sqrt{1 - 6a\zeta(5\lambda^2)^{-1}}], \quad (8)$$

which is real for $a < a_+$, where $a_+ = 5\lambda^2/6\zeta$. This gives a condition of existence of the Hex-B phase. In turn, assuming a small difference Δn between n_{Sm} and n_H , $n_H = n_{Sm} - \Delta n$, and minimizing expression (7) with respect to the order

parameter ψ , from Eq. (6) we obtain

$$\Delta n = \frac{\partial a}{\partial n} \left(\frac{\partial \mu}{\partial n} \right)^{-1} |\psi|^2, \quad (9)$$

where $\mu = \partial \varphi / \partial n$ and where we discard high orders of $|\psi|^2$. Upon diminishing T the parameter a monotonically decreases and turns to zero. At this point $a = 0$ the smectic phase becomes absolutely unstable. Thus, from condition $0 < a < a_+$ one can find that the equilibrium between Hex- B and Sm- A phases occurs in bulk in the interval

$$\Delta T = \frac{5\lambda^2}{6\alpha\zeta} T_0. \quad (10)$$

To take surface effects into account, one should include the gradient term into the Landau functional for the field ψ (per unit volume). Then we obtain for the Landau functional of the film

$$\mathcal{F} = S \int_{-L/2}^{L/2} dz \{ b (\partial_z \psi)^2 + g[\psi] \}, \quad (11)$$

where $b > 0$, the z axis is perpendicular to the film, and $z = \pm L/2$ correspond to free surfaces of FSF of thickness L and surface area S . We assume in the following that the phase of the hexatic order parameter ψ is fixed, and therefore one can use real values of ψ . Due to the symmetry properties of FSF we have condition $\partial_z \psi[0] = 0$ in the middle of the film. Minimization of Eq. (11) with respect to ψ gives a Euler-Lagrange equation, which can be integrated once to yield

$$b(\partial_z \psi)^2 = g[\psi] + C_1, \quad (12)$$

where $C_1 = -g[\psi_m]$, $\psi[z=0] \equiv \psi_m$. At $z \rightarrow 0$ the solution for $\psi[z]$ approaches its asymptotic bulk value, i.e., $\psi_m \approx \psi_H$ in the Hex- B phase and $\psi_m \approx 0$ in the Sm- A phase. In the above we have used the assumption $L \gg \xi_z$, which is true for the thick FSF under consideration. Here $\xi_z = \sqrt{b/(\alpha\tau)}$ is the hexatic correlation length along the z axis, which is much larger than the molecular size close to the TCP.

There are two contributions to the Landau functional of the film \mathcal{F} : the bulk energy $\mathcal{F}^{(b)} = g[\psi_H]LS$ and surface energy $\mathcal{F}^{(s)}$. The last one can be found after subtracting $\mathcal{F}^{(b)}$ from expression (11). With the use of Eq. (12) we can obtain

$$\mathcal{F}^{(s)} = 2bS \int_{-L/2}^{L/2} dz (\partial_z \psi)^2. \quad (13)$$

Assuming that $\psi^{(s)} \gg \psi_H$ [44], where $\psi^{(s)}$ is the surface value of ψ , it follows from Eqs. (7) and (12) that in both phases there exists a region near the surface where ψ^6 becomes a leading term on the right-hand side of Eq. (12), i.e., it can be written as

$$b(\partial_z \psi)^2 = \zeta \psi^6 / 90. \quad (14)$$

In this case the solution of Eq. (14) gives the following dependence for ψ^2 within a region near the surface (for $z > 0$):

$$\psi^2 \approx \frac{(\psi^{(s)})^2}{1 + (\psi^{(s)})^2 \sqrt{2\zeta/(45b)}(L/2 - z)} \left(\text{for } \frac{L}{2} - z \ll \frac{2\sqrt{2b\zeta}}{\sqrt{5}\lambda} \right), \quad (15)$$

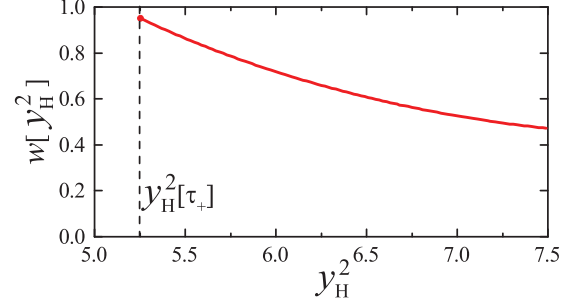


FIG. 5. Dependence of the function $w[y_H^2]$ on y_H^2 for the typical values of material constants $\alpha = 10^8 \text{ J m}^{-3}$, $\lambda = 2 \times 10^3 \text{ J m}^{-3}$, $\zeta = 10^7 \text{ J m}^{-3}$, and $b = 10^{-14} \text{ J m}^{-1}$. The simulations were performed for $\psi_H^{(s)} = 4.52\psi_H$ and $\psi_{Sm}^{(s)} = 2.52\psi_H$. The region of real values of ψ_H is located on the right side from the vertical dashed line, $\tau_+ = a_+/\alpha$.

which is valid for both phases. The surface value of ψ is denoted for the Hex- B and Sm- A phases as $\psi_H^{(s)}$ and $\psi_{Sm}^{(s)}$, respectively ($\psi_H^{(s)} > \psi_{Sm}^{(s)}$). These values should be substituted in Eq. (15) to obtain the corresponding z dependencies of ψ^2 for each of the phases.

The analysis of the solution of Eq. (12) indicates that even in the Sm- A phase the hexatic order diminishes from its surface magnitude to a value $\sim \psi_H/2$ within an extended range $\sim \xi_z \ln[\tau - \tau_c]$. This is a manifestation of an essential increase of the penetration length of hexatic ordering in FSF close to TCP.

Substituting the above solution into Eq. (13) one obtains main contributions to the surface energy. Using expressions (13) and (12) one finds the difference between the surface energies of the Hex- B and Sm- A phases

$$\frac{\Delta \mathcal{F}^{(s)}}{4\sqrt{b}S} = \int_{\psi_H^{(s)}}^{\psi_H^{(s)}} d\psi \sqrt{g[\psi] - g[\psi_H]} - \int_0^{\psi_{Sm}^{(s)}} d\psi \sqrt{g[\psi]}. \quad (16)$$

Using equation $\partial g[\psi_H]/\partial \psi_H = 0$, we obtain from Eq. (16)

$$\Delta \mathcal{F}^{(s)} = (b\zeta)^{1/2} w[\psi_H^2 \zeta / \lambda] \psi_H^4 S, \quad (17)$$

where $w[\psi_H^2 \zeta / \lambda]$ is a dimensionless function that depends on the surface values of ψ . The exact values of ψ can be obtained only numerically [$\psi_H^2 \zeta / \lambda \sim 1$ as follows from Eq. (8)]:

$$w[y_H^2] = 4\sqrt{\frac{5}{3}} \left\{ 5 \left[1 + \sqrt{1 - \frac{2}{5} y_H^2 \left(1 - \frac{y_H^2}{10} \right)} \right] \right\}^{-3/2} \times \left\{ \int_{y_H}^{y_H^{(s)}} dy \sqrt{\tilde{g}[y] - \tilde{g}[y_H]} - \int_0^{y_{Sm}^{(s)}} dy \sqrt{\tilde{g}[y]} \right\}, \quad (18)$$

where $y^2 = \psi^2 \zeta / \lambda$ ($y_H^2 = \psi_H^2 \zeta / \lambda$),

$$\tilde{g}[y] = \left\{ 1 - \frac{y^2}{10} \right\} y^2 - \frac{y^4}{2y_H^2} + \frac{y^6}{30y_H^2}. \quad (19)$$

The typical dependence of the function $w[y_H^2]$ on its argument containing several hexatic parameters is presented in Fig. 5.

Comparing the difference between the surface energies of the Hex- B and Sm- A phases in Eq. (17) with the bulk

energy $\mathcal{F}^{(b)}$ we conclude that surface effects produce an effective positive correction $\delta\lambda \simeq 6(b\zeta)^{1/2}w[\psi_H^2\zeta/\lambda]L^{-1}$ to the coefficient λ . Using Eq. (10) we finally arrive to

$$\Delta T = \frac{5\lambda^2}{6\alpha\zeta} T_0 \left(1 - \frac{L_0}{L}\right)^2, \quad (20)$$

where

$$L_0 = \frac{6(b\zeta)^{1/2}}{\lambda} w[\psi_H^2\zeta/\lambda] \quad (21)$$

is a characteristic length scale. Equation (20) is valid for the film thickness $L \gg L_0$. Fitting of the experimental data with Eq. (20) shows good agreement with theoretical predictions (see Fig. 4), and gives $L_0 = 0.9 \mu\text{m}$. As soon as the value of $w[\psi_H^2\zeta/\lambda]$ is of the order of unity, it follows from Eq. (21) that the value of L_0 is determined by the hexatic correlation length along the z axis [one can see from above that $\xi_z \sim \sqrt{b/(\alpha\tau_c)} \simeq \sqrt{b\zeta}/\lambda$, which is the main factor in Eq. (21)], which has to be much larger than the molecular length ($\sim 3 \times 10^{-9}$ m) close to the TCP, i.e., by more than two orders of magnitude.

V. CONCLUSIONS

In conclusion, we report detailed spatially resolved x-ray studies of a first-order Sm-A–Hex- B phase transition in freestanding films of 54COOBC of various thickness. Microfocused x-ray diffraction in combination with the XCCA technique allowed us to directly observe the coexistence of the Sm-A and Hex- B phases. Experimentally measured temperature dependence of such structural parameters as C_6 , ξ , and q_0 exhibits discontinuous behavior at the transition temperature, which was not observed for the second-order Sm-A–Hex- B phase transition in other compounds [26]. We also found that the width of the two-phase coexistence region ΔT at

the Sm-A–Hex- B transition becomes narrower for thinner films, reaching the value of about 500 mK for a 2- μm -thick film. This indicates that the phase behavior of the 54COOBC films is strongly affected by the surface hexatic ordering field, which penetrates into interior layers of the film over large distances induced by the proximity of the Sm-A–Hex- B transition in 54COOBC to a TCP. An analytical expression for ΔT obtained from the Landau mean-field theory is in good agreement with the experimental data. This gives a unique possibility to approach TCP at the Sm-A–Hex- B phase transition line by varying the film thickness and experimentally investigating general properties of the phase transitions in the vicinity of the TCP. This approach is quite general and can be applied to a large class of systems exhibiting TCPs, for example, helimagnetic films [45], or recently discovered materials with skyrmionic magnetic lattices [12,13].

ACKNOWLEDGMENTS

We acknowledge E. Weckert for fruitful discussions and support of the project, F. Westermeister for support during the experiment, A. R. Muratov for theoretical discussions, and R. Gehrke for careful reading of the manuscript. The work of R.M.K., E.S.P., and B.I.O. was supported by the Russian Science Foundation (Grant No. 18-12-00108). N.A.C. acknowledges the support of US National Science Foundation Grants No. DMR1420736 and No. DMR1710711. The work of V.V.L. and E.I.K. was supported by the Ministry of Science and Higher Education of Russia within the State assignment (theme No. 0033-2018-0003, Reg. No. AAAA-A18-118042790132-2). The work of I.A.Z., R.P.K., N.M., Y.Y.K., and I.A.V. was supported by the Helmholtz Association's Initiative and Networking Fund and the Russian Science Foundation (Project No. 18-41-06001).

-
- [1] P. Chaikin and T. Lubensky, *Principles of Condensed Matter Physics* (Cambridge University Press, Cambridge, 1995).
 - [2] B. Fultz, *Phase Transitions in Materials* (Cambridge University Press, Cambridge, 2014).
 - [3] P. de Gennes and J. Prost, *The Physics of Liquid Crystals*, 2nd ed. (Oxford University Press, New York, 1993).
 - [4] P. Bolhuis and D. Frenkel, *Phys. Rev. Lett.* **72**, 2211 (1994).
 - [5] E. Styk, W. Rzyzsko, and P. Bryk, *J. Chem. Phys.* **141**, 044910 (2014).
 - [6] Y. Lee, S. Jo, W. Lee, H. Lee, Y. S. Han, and D. Y. Ryu, *Polymer* **112**, 427 (2017).
 - [7] S. Mao, Q. MacPherson, and A. J. Spakowitz, *Phys. Rev. Lett.* **120**, 067802 (2018).
 - [8] J. Thoen, H. Marynissen, and W. Van Dael, *Phys. Rev. Lett.* **52**, 204 (1984).
 - [9] B. M. Ocko, R. J. Birgeneau, J. D. Litster, and M. E. Neubert, *Phys. Rev. Lett.* **52**, 208 (1984).
 - [10] M. A. Anisimov, P. E. Cladis, E. E. Gorodetskii, D. A. Huse, V. E. Podneks, V. G. Taratuta, W. van Saarloos, and V. P. Voronov, *Phys. Rev. A* **41**, 6749 (1990).
 - [11] A. Bauer, M. Garst, and C. Pfeleiderer, *Phys. Rev. Lett.* **110**, 177207 (2013).
 - [12] M. Garst, J. Waizner, and D. Grundler, *J. Phys. D: Appl. Phys.* **50**, 293002 (2017).
 - [13] J. Mulkers, K. M. D. Hals, J. Leliaert, M. V. Milošević, B. Van Waeyenberge, and K. Everschor-Sitte, *Phys. Rev. B* **98**, 064429 (2018).
 - [14] P. Oswald and P. Pieranski, *Smectic and Columnar Liquid Crystals* (Taylor & Francis, Boca Raton, 2006).
 - [15] W. H. de Jeu, B. I. Ostrovskii, and A. N. Shalaginov, *Rev. Mod. Phys.* **75**, 181 (2003).
 - [16] D. R. Nelson, *Defects and Geometry in Condensed Matter Physics* (Cambridge University Press, Cambridge, 2002).
 - [17] J. M. Kosterlitz, *Rep. Prog. Phys.* **79**, 026001 (2016).
 - [18] L. Agosta, A. Metere, and M. Dzugutov, *Phys. Rev. E* **97**, 052702 (2018).
 - [19] R. Pindak, D. E. Moncton, S. C. Davey, and J. W. Goodby, *Phys. Rev. Lett.* **46**, 1135 (1981).
 - [20] J. D. Brock, A. Aharony, R. J. Birgeneau, K. W. Evans-Lutterodt, J. D. Litster, P. M. Horn, G. B. Stephenson, and A. R. Tajbakhsh, *Phys. Rev. Lett.* **57**, 98 (1986).

- [21] T. Stoebe and C. C. Huang, *Int. J. Mod. Phys. B* **9**, 2285 (1995).
- [22] L. D. Landau and E. M. Lifshitz, *Course of Theoretical Physics, Statistical Physics, Part 1* (Pergamon Press, New York, 1980).
- [23] A. J. Jin, M. Veum, T. Stoebe, C. F. Chou, J. T. Ho, S. W. Hui, V. Surendranath, and C. C. Huang, *Phys. Rev. E* **53**, 3639 (1996).
- [24] H. Haga, Z. Kutnjak, G. S. Iannacchione, S. Qian, D. Finotello, and C. W. Garland, *Phys. Rev. E* **56**, 1808 (1997).
- [25] R. P. Kurta, B. I. Ostrovskii, A. Singer, O. Y. Gorobtsov, A. Shabalin, D. Dzhigaev, O. M. Yefanov, A. V. Zozulya, M. Sprung, and I. A. Vartanyants, *Phys. Rev. E* **88**, 044501 (2013).
- [26] I. A. Zaluzhnyy, R. P. Kurta, E. A. Sulyanova, O. Y. Gorobtsov, A. G. Shabalin, A. V. Zozulya, A. P. Menushenkov, M. Sprung, A. Krowczynski, E. Gorecka, B. I. Ostrovskii, and I. A. Vartanyants, *Soft Matter* **13**, 3240 (2017).
- [27] B. Van Roie, K. Denolf, G. Pitsi, and J. Thoen, *Eur. Phys. J. E* **16**, 361 (2005).
- [28] F. Mercuri, S. Paoloni, M. Marinelli, R. Pizzoferrato, and U. Zammit, *J. Chem. Phys.* **138**, 074903 (2013).
- [29] A. J. Jin, M. Veum, T. Stoebe, C. F. Chou, J. T. Ho, S. W. Hui, V. Surendranath, and C. C. Huang, *Phys. Rev. Lett.* **74**, 4863 (1995).
- [30] C.-F. Chou, J. T. Ho, S. W. Hui, and V. Surendranath, *Phys. Rev. Lett.* **76**, 4556 (1996).
- [31] C.-F. Chou, A. J. Jin, S. W. Hui, C. C. Huang, and J. T. Ho, *Science* **280**, 1424 (1998).
- [32] V. Surendranath, D. L. Fishel, A. de Vries, R. Mahmood, and D. L. Johnson, *Mol. Cryst. Liq. Cryst.* **131**, 1 (1985).
- [33] I. A. Zaluzhnyy, R. P. Kurta, E. A. Sulyanova, O. Y. Gorobtsov, A. G. Shabalin, A. V. Zozulya, A. P. Menushenkov, M. Sprung, B. I. Ostrovskii, and I. A. Vartanyants, *Phys. Rev. E* **91**, 042506 (2015).
- [34] P. Wochner, C. Gutt, T. Autenrieth, T. Demmer, V. Bugaev, A. D. Ortiz, A. Duri, F. Zontone, G. Grübel, and H. Dosch, *Proc. Natl. Acad. Sci. USA* **106**, 11511 (2009).
- [35] M. Altarelli, R. P. Kurta, and I. A. Vartanyants, *Phys. Rev. B* **82**, 104207 (2010); **86**, 179904(E) (2012).
- [36] R. P. Kurta, M. Altarelli, and I. A. Vartanyants, *Adv. Condens. Matter Phys.* **2013**, 959835 (2013).
- [37] R. P. Kurta, M. Altarelli, and I. A. Vartanyants, in *Advances in Chemical Physics* (Wiley, New York, 2016), Vol. 161, Chap. 1, pp. 1–39.
- [38] J. Brock, D. Noh, B. McClain, J. Litster, R. Birgeneau, A. Aharony, P. Horn, and J. Liang, *Z. Phys. B: Condens. Matter* **74**, 197 (1989).
- [39] T. Stoebe, R. Geer, C. C. Huang, and J. W. Goodby, *Phys. Rev. Lett.* **69**, 2090 (1992).
- [40] I. A. Zaluzhnyy, R. P. Kurta, A. P. Menushenkov, B. I. Ostrovskii, and I. A. Vartanyants, *Phys. Rev. E* **94**, 030701 (2016).
- [41] G. Aeppli and R. Bruinsma, *Phys. Rev. Lett.* **53**, 2133 (1984).
- [42] S. C. Davey, J. Budai, J. W. Goodby, R. Pindak, and D. E. Moncton, *Phys. Rev. Lett.* **53**, 2129 (1984).
- [43] A. Z. Patashinskii and V. L. Pokrovskii, *Fluctuation Theory of Phase Transitions* (Pergamon Press, Oxford, 1979).
- [44] The bulk value of the hexatic order parameter in the Sm-A phase is zero, and near the TCP it is small in the Hex-B phase. However, experimental data in Sm-A FSFs [46–49] suggest that the surface value of the hexatic order parameter is much larger than its bulk value. Simulations performed in this work were made under this assumption.
- [45] M. Janoschek, M. Garst, A. Bauer, P. Krautscheid, R. Georgii, P. Böni, and C. Pfeleiderer, *Phys. Rev. B* **87**, 134407 (2013).
- [46] E. B. Sirota, P. S. Pershan, S. Amador, and L. B. Sorensen, *Phys. Rev. A* **35**, 2283 (1987).
- [47] S. Amador, P. S. Pershan, H. Stragier, B. D. Swanson, D. J. Tweet, L. B. Sorensen, E. B. Sirota, G. E. Ice, and A. Habenschuss, *Phys. Rev. A* **39**, 2703 (1989).
- [48] R. Geer, T. Stoebe, and C. C. Huang, *Phys. Rev. E* **48**, 408 (1993).
- [49] W. H. de Jeu, A. Fera, O. Konovalov, and B. I. Ostrovskii, *Phys. Rev. E* **67**, 020701 (2003).